Colloids and Surfaces A: Physicochem. Eng. Aspects 463 (2014) 110–117

Contents lists available at ScienceDirect

Colloids and Surfaces A: Physicochemical and Engineering Aspects

journal homepage: www.elsevier.com/locate/colsurfa

Preparation of functional currant-bun-like fumed silica/polymethacrylate nanoparticles by radiation-induced polymerization

Leandro J. Martínez [a], Mirna L. Sánchez [a], Pamela Kikot [a], Roberto Candal [b], Mariano Grasselli [a,*]

[a] LaMaBio, Laboratorio de Materiales Biotecnológicos, Depto. de Ciencia y Tecnología, Universidad Nacional de Quilmes – IMBICE (CONICET), Roque Sáenz Peña 352, B1876BXD Bernal, Argentina
[b] Instituto de Fisicoquímica de Materiales Ambiente y Energía, CONICET, FCEN-UBA, Ciudad Universitaria, Pabellón II, 1428 Buenos Aires, Argentina

HIGHLIGHTS

- Colloidal composites based on fumed silica and polymethacrylate are prepared.
- Nanocomposites are obtained by radiation-induced polymerization under non-stirring.
- Currant-bun-like nanoparticles can be size-tuned according to the initial reagents.
- Reversible protein adsorptive properties are studied onto sulfonic nanocomposites.
- Potential applications as protein-capture materials are envisioned.

GRAPHICAL ABSTRACT

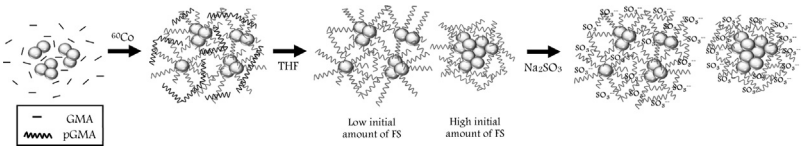

ARTICLE INFO

Article history:
Received 18 July 2014
Received in revised form 9 September 2014
Accepted 11 September 2014
Available online 19 September 2014

Keywords:
Nanosilica
Glycidyl methacrylate
Gamma rays
Protein adsorption

ABSTRACT

Fumed silica (FS) is one of the few nanomaterials used in large scale in the production of several industrial products. In addition, the very low toxicity of these nano-sized particles led them to become excellent raw materials to develop novel applications in the field of downstream processing of bioproducts. In this work, we prepared and characterized a colloidal composite based on fumed silica with protein adsorption properties. This nanocomposite was prepared by radiation-induced polymerization of glycidyl methacrylate (GMA) dissolved in an aqueous suspension of FS without stirring. According to the initial GMA/FS ratio, mono-disperse nanoparticles from 60 to 195 nm were obtained. Sulfonic nanoparticles allowed reversible lysozyme adsorption up to 270 mg/g. The nanomaterials prepared have potential application as protein-capture materials in the field of downstream processing of proteins.

1. Introduction

Fumed silica (FS) is one of the few nanomaterials used in large scale in the production of several industrial products. This nanomaterial is used as a universal thickening agent and anticaking agent in powders and also as a desiccant. In addition, it has many applications in massive products such as cosmetics, for its light-diffusing

* Corresponding author. Tel.: +54 1143657100x5624; fax: +54 1143657132.
E-mail addresses: mariano.grasselli@unq.edu.ar, mariano.grasselli@gmail.com (M. Grasselli).

http://dx.doi.org/10.1016/j.colsurfa.2014.09.015
0927-7757/

properties, and toothpaste, for its light abrasive capability. FS is also used as filler in silicone elastomer and as a viscosity adjuster in paints, coatings, printing inks, adhesives and unsaturated polyester resins. However, our main interest in this material is its low toxicity. This feature allows it to be used as food additive to improve the organoleptic properties of massive food products.

Among the numerous inorganic/organic composite materials, silica/polymer composites are the most commonly reported [1,2]. Silica particles are used mainly in polymer composites to improve their mechanical properties and in neat polymers to protect their optical clarity [3].

Colloidal silica/polymer composites are a new category of nanocomposites, which can be divided in polymer core and silica shell or vice versa [4]. In this work, we were interested in nanoparticles (NPs) with a functional polymer shell available to interact with the medium. These nanocomposites can be prepared in different morphologies, such as raspberry-like, currant-bun-like or core–shell arrangements depending on the surface chemistry and the size of the inorganic particles [5]. The chemical functionalization of these colloidal composites is technologically interesting due to their potential to be used as protein-capture materials in the biotechnology field.

The modern biotech industry depends heavily on the availability of efficient processes that can generate competitive products or services in terms of quality and cost. The significant advances in fermentation technologies in the last 20 years have not been corresponded by those in the downstream processing (DSP) of bioproducts [6]. The DSP, which can account for up to 80% of the production costs, is currently the main bottleneck in bioproduct generation. The application of NPs to the DSP attracts the attention of the research community because of the high surface area of these materials, which may allow overcoming the restriction of the low-capacity adsorption of the micron-size adsorption materials. For example, magnetic microparticles, which have maximum protein adsorption capacities between 1 and 10 mg/mL, are currently used in bioresearch laboratories to isolate small amounts of proteins. In contrast, functional magnetic NPs have shown higher specific protein adsorption capacity (one order of magnitude higher) than commercial magnetic microparticles [7,8]. Also, the elimination of mass-transport limitations due to diffusion within the beads reduces the capture time to a few minutes. Recently, a novel technical-scale continuous protein recovery process, based on magnetic NPs, has been used to isolate biologically active compounds directly from crude culture media [9]. However, the high cost of these magnetic carriers and adsorbents has been pointed out as one of the main restrictions for their application in industrial processes [10]. Therefore, simple and inexpensive materials should be developed to allow NP applications in the field of DSP of bioproducts.

Other difficulties coming with the reduction of the particle size are the suspect of toxicity of nanomaterials [11] and, from the bioprocessing point of view, the need to find out efficient methods to isolate them after the adsorption step. Typically, the adsorptive microbeads of polymers applied in the DSP have a density near that of water, which combined with a nanometer-sized diameter, impairs the use of centrifugation as a solid–liquid operation unit. Inorganic cores of core–shell composite NPs could be an alternative to increase NP separation feasibility by magnetic or centrifugal forces. In this way, ferric oxide colloidal composites have been successfully applied to laboratory-scale protein purification, using magnetic separation [7,8,10]. However, concerns about the toxicity of metal pieces, at the nanoscale range, are an issue in the development of protein-adsorption materials for DSP and application in the biomedical field [11,12].

Silica material has a bulk density of 2.2 g/mL and the toxicity of silica nano-sized particles is very low [13,14]. In addition, they are considered as GRAS food additive by the FDA. Also, amorphous silica matrices have been shown to be non-toxic and biologically inert for mammalian cells in aqueous environments [15].

Table 1
Composition of samples for preparation of the composites previously to the polymerization induced by gamma ray irradiation.

Sample	FS (mg)	FS-stock suspension (mL)	GMA (mg)	H_2O (mL)
FS2/pGMA	22.5	0.45	0.5	145.1
FS9/pGMA	90	1.8	0.5	131.6
FS27/pGMA	270	5.4	0.5	95.6
FS54/pGMA	540	10.8	0.5	41.6

Silica particles have usually been associated with polyacrylates, particularly poly(methylmethacrylate) [1,4,16]. Poly(glycidylmethacrylate) (pGMA) shares similar physical properties with poly(methylmethacrylate), such as film forming, and good mechanical properties [17,18]. However, from the chemical point of view, pGMA has a significant advantage because of the chemical reactivity of its pendant oxirane rings, which can be used to introduce different functionalities [19]. Composite NPs containing pGMA may be able to functionalize with ligands by simple methods, reaching stable chemistry and using low-cost reagents [20,21].

The objective of this work was to prepare and characterize a novel colloidal FS/pGMA nanocomposite, with specific protein adsorption properties for potential application in the field of DSP of bioproducts.

2. Materials and methods

Fumed silica (FS), with an average particle diameter of 14 nm (information provided by the supplier), glycidyl methacrylate ≥ 97.0% (GMA), and tetrahydrofuran (THF) for synthesis were from Sigma Chemical Co. (USA), and were used without further purification. Lysozyme (Hansozyme) was kindly donated by Christian Hansen Argentina. Deionized and filtered water (0.22 μm filter) was used through all the processes. All other chemicals used were of analytical grade.

The colloidal FS/pGMA nanocomposite was prepared by the graft polymerization technique induced by ionizing radiation, using a ^{60}Co gamma source. A stock suspension of FS (50 mg/mL in water) was previously prepared by stirring with vortex. The composition of the different samples before radiation is described in Table 1. Glass vials (20 mL) containing GMA monomer and the respective FS suspension were flushed with nitrogen and sealed hermetically. To disperse reagents, samples were first treated with a vortex mixer (Thermolyne Type 37600 Mixer) for 30 s and then placed in an ultrasonic bath for 30 min (TESLAB model TB02 – TACA, 80 W power, 40 kHz). It is noteworthy that, under these experimental conditions, GMA is completely soluble in the mixture.

Samples were irradiated at room temperature in a semi-industrial ^{60}Co source (PISI, CNEA-Ezeiza, Argentina). Samples received an average dose of 10 kGy at a rate of 1 kGy/h. After irradiation, composite suspensions were treated with THF for homopolymer extraction. For this purpose, the supernatant was completely removed, and 10 mL of THF was added to the glass vial. The extraction procedure was allowed shaking overnight at room temperature. Finally, vials were allowed to settle for 60 min. Precipitates were discarded and the residual THF was removed from the suspension in a SpeedVac concentrator (Savant SpeedVac AES2010 Centrifugal Evaporator-220). Each sample was fractionated into low volume and concentrated for 3 h without heating, until the sample was reduced to 0.500 mL. Then, each tube was filled back to 2 mL with water. To assure complete THF evaporation, the cycle

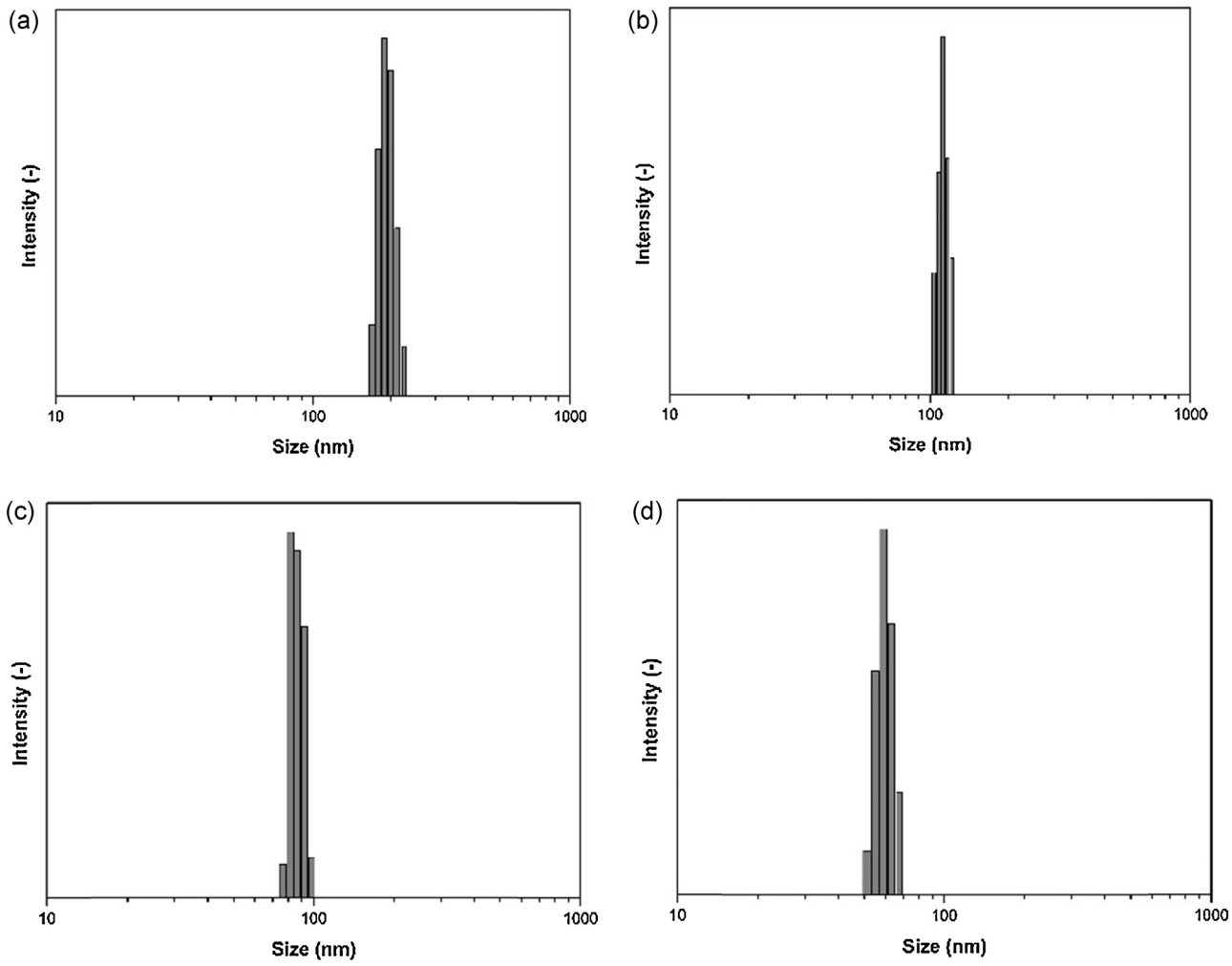

Fig. 1. Particle size distribution of colloidal composite NP according DLS measurements. (a) FS2/pGMA; (b) FS9/pGMA; (c) FS27/pGMA; (d) FS54/pGMA.

was repeated twice. Finally, the suspension was allowed to settle for 60 min and homopolymer traces were removed as precipitate.

The relative composition of polymethacrylate of the colloidal FS/pGMA nanocomposite was determined by thermal gravimetric analysis (TGA), based on the percentage of weight loss from 150 to 700 °C, corresponding to the decomposition of organic matter, in this case from pGMA.

The materials were analyzed by spectroscopic and functional techniques. Shimadzu FTIR IRAffinity equipped with GladiATR (PIKE Technologies, Inc.) module was used to determine the presence of the polymer in the polymer nanocomposites. The FTIR spectra, which averaged 64 scans, were analyzed using the IRsolution software. The average diameter of the nanocomposites was determined by dynamic light scattering (DLS) in a 90 Plus – Particle Size Analyzer (Brookhaven Instruments Corporation). The measurements were performed at 25 °C on samples diluted in deionized and filtered water. Each result was the average of three consecutive measurements of 30 s each.

Thermal analysis of the samples was carried out by using thermal gravimetric analysis (TGA) (TA Instruments Q500) under a nitrogen atmosphere with a heating rate of 10 °C/min, from 25 to 800 °C.

The structure of the NPs was visualized by a Field Emission Scanning Electron Microscope (FSEM) Carl Zeiss NTS-40 using 3.0 kV SUPRA energy. The zeta potential of the colloidal NPs was measured with a Brookhaven 90 Plus/Bi-MAS, operating at $\lambda = 635$ nm, 15 mW, with a solid state laser, a measurement angle of 90° and at 25 ± 0.1 °C. The suspensions were diluted in KCl 0.03 M as supporting electrolyte and equilibrated at various pH values by adding HCl or KOH. Prior to measurement, the samples were sonicated for 15 min.

Cation-exchange NPs were prepared from colloidal FS/pGMA by ring-opening reaction with sodium sulfite, as previously described [22], with the addition of a stabilizer. Briefly, one part of the FS/pGMA NP suspension and three parts of sulfite mixture (sodium sulfite/isopropyl alcohol/water 10/15/75, w/w/w) were incubated overnight at 40 °C under shaking (100 rpm). Five percent of 1 N sodium hexametaphosphate was added as surfactant agent to the reaction mixture.

Sulfonic colloidal NP composites (S-FS/pGMA NPs) were washed by three centrifugation/resuspension cycles with water in a Hermle Z200 M/H centrifuge, at 12,000 × *g* for 3 min. The final washing step was performed with 50 mM phosphate buffer pH 7.

S-FS/pGMA NPs were used as adsorbent material. Adsorption/desorption experiments were carried out in triplicate with different concentrations of lysozyme, according to the capacity of the adsorbent material. The adsorption study was performed by the following sequential steps: equilibration, loading, washing and elution steps. The lysozyme concentration was determined by absorbance at 280 nm and using the extinction coefficient 2.4 mL/(g cm^{-1}). Assays were performed in Eppendorf tubes with approximately 250 mg of S-FS/pGMA NPs. The tubes were preweighed to calculate the amount of NPs by dry weight. The adsorption process began with S-FS/pGMA NP equilibration with

Table 2
Particle diameter determined by DLS of FS/pGMA colloidal composite prepared by radiation-induced polymerization.

Sample	Particle diameter (nm)
FS2/pGMA	195 ± 13
FS9/pGMA	120 ± 7
FS27/pGMA	90 ± 8
FS54/pGMA	60 ± 8

50 mM phosphate buffer, pH 7. After 15 min, the suspension was centrifuged and the supernatant discarded. The pellet of the S-FS/pGMA NPs was disrupted and incubated with an aqueous solution of lysozyme (15 mg/mL maximum) for 45 min. After centrifugation, protein concentration was measured by a UV–vis spectrophotometer at 280 nm in the supernatant (non-adsorbed protein). After three washing cycles (centrifugation/resuspension) with 50 mM phosphate buffer, pH 7, the elution step was carried out with 50 mM phosphate buffer pH 7, 1 M NaCl. Finally, the S-FS/pGMA NPs were dried at 60 °C to constant weight. Maximum adsorption capacity (Ads_{max}) was calculated as the amount of lysozyme removed from the initial protein solution per dry weight of NPs, whereas the maximum binding capacity (Q_{max}) was calculated as the amount of lysozyme recovered in the elution step per dry weight of NPs.

3. Results and discussion

The most frequent method to prepare colloidal NP composites is the in situ heterophase polymerization, where the polymer encapsulates silica NPs. It is recognized that surface-initiated polymerization methods are able to prepare structurally well-defined polymer/silica nanocomposites [23]. Whichever preparative method is used, synthetic procedures commonly require a significant affinity between silica surfaces and polymers. The general approach involves two successive steps: (i) synthesis of the core material with the desired surface group and chemical reactivity and (ii) coating of the template core with an organic or inorganic shell to establish a physicochemical or chemical link between the constituents [24]. However, under defined conditions, the first step can be a simple physical adsorption of the monomer or initiator to silica NPs. In this way, aqueous surfactant-free synthesis of vinyl polymer/silica colloidal nanocomposites has been reported by copolymerization of 4-vinylpyridine with either n-butyl acrylate or n-butyl methacrylate in the presence of an ultrafine aqueous silica solution [25]. This polymerization method is carried out under stirring in a nitrogen atmosphere, and ammonium persulfate initiator at 60 °C. In this work, similar sample preparations were set up to prepare surfactant-free colloidal FS/pGMA NPs. GMA was added to the aqueous suspension of FS and sealed under a nitrogen atmosphere in a glass vial. The polymerization reaction was initiated by irradiation in a ^{60}Co source without stirring at room temperature.

GMA has low water solubility (5 g/L a 20 °C). Therefore, preliminary experiments were done to select the proper GMA concentration, in order to maintain the monomer soluble and to reach a stable suspension after irradiation. FS was set at 50 mg/mL and different amounts of GMA (0 mM, 2 mM, 5 mM, 10 mM, 20 mM, 50 mM and 100 mM) were added to the FS suspension. Samples with 20 mM or lower GMA concentrations had a particle-like aspect after irradiation. Higher GMA concentrations yielded unwanted gel-like products. In addition, samples prepared using 20 mM GMA led to homogeneous suspensions at naked eye, before irradiation. Therefore, this GMA concentration was used for further experiments and FS concentration was varied in a wide range (see Table 1). The amount of FS required for each condition was achieved from a

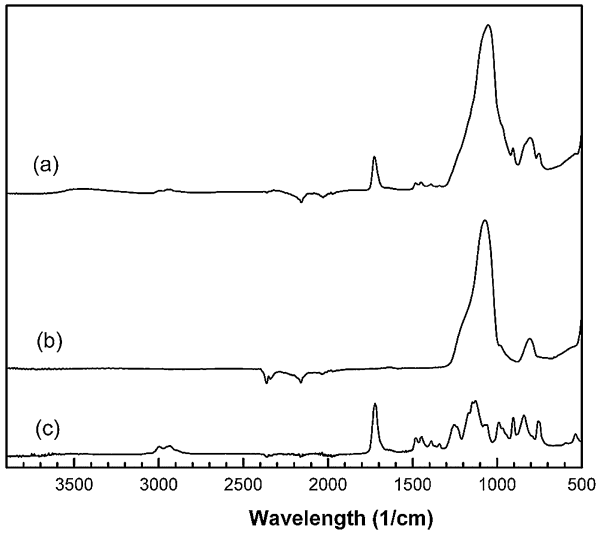

Fig. 2. Infrared analysis of dry samples of (a) FS2/pGMA; (b) fumed silica and (c) pGMA.

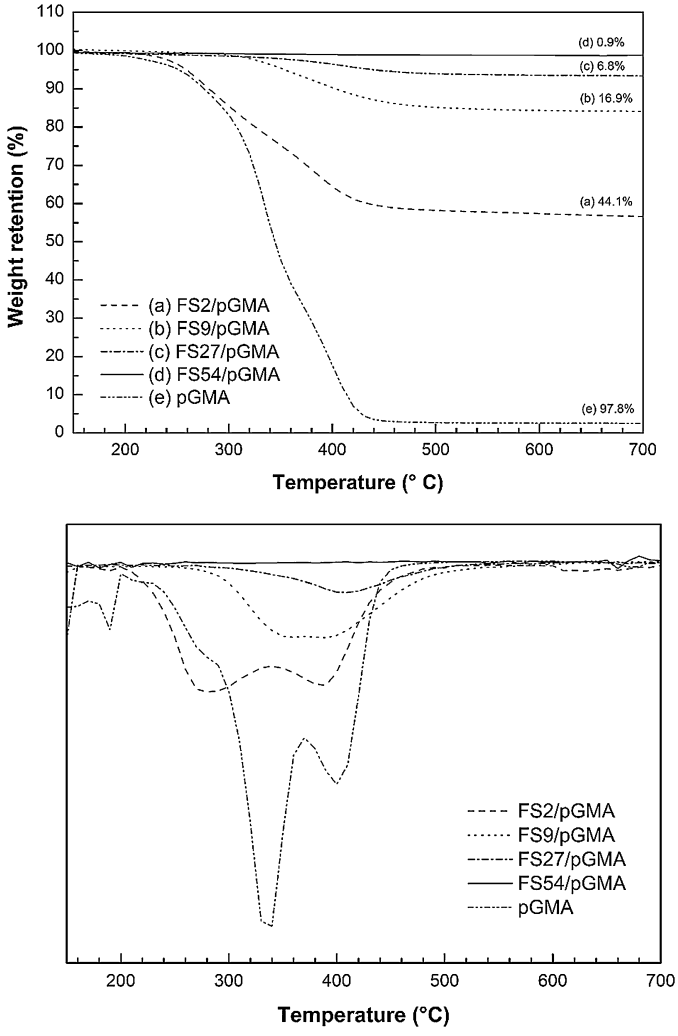

Fig. 3. Thermogravimetric analysis of samples. Weight retention percentage as function of temperature, heating rate of 10 °C/min (upper plot). Derivative of weight retention percentage as function of temperature plot (lower plot). Samples: (a) FS2/pGMA; (b) FS9/pGMA; (c) FS27/pGMA; (d) FS54/pGMA and (e) pGMA.

concentrated aqueous suspension (50 mg/mL), where each condition was named by the initial amount of FS.

Free-radical polymerizations of (meth)acrylates are usually initiated by heat and UV light to prepare poly(meth)acrylates. However, radiation-induced polymerization is an alternative method with some advantages: it is a temperature-independent process, it creates a much larger amount of free radicals in a highly homogeneous and quantitatively manner [26] and it has the ability to generate radicals onto very stable materials, such as polyethylene, which allows grafting polymerization [27]. The radiolytic approach may offer some advantages in the fine control over the rate of generation of the growing species afforded by the control over the dose rate delivered to the sample [28].

Gamma-irradiation of silica NP suspensions (up to 20 nm in diameter) has been previously studied by Meisel [29]. These authors found that the addition of silica NPs to water up to 50% did not change the radiolytic yields of radicals and interfacial exchange of charge carriers between the solid particle and the aqueous phase. In contrast, the presence of the solid phase often enhanced products from the fragmentation of water molecules. They concluded that the production of radicals at the interface may be used for a variety of processes such as polymerization at the surface or grafting onto the solid [29]. They also observed that the mobility of hot holes in silica is much slower than that of electrons, and that, thus, the latter escape into the aqueous phase, yielding additional radicals [29].

In this work, the irradiation dose was set at 10 kGy and the dose rate at 1 kGy/h, which generate enough electrons to convert all GMA in polymethacrylate in this solvent [30]. After irradiation, samples were treated with THF, a moderately polar heterocyclic solvent capable of dissolving a wide range of organic compounds, to remove the homopolymer. Finally, THF was changed by water using the SpeedVac, avoiding the complete sample dryness, to reduce NP aggregation.

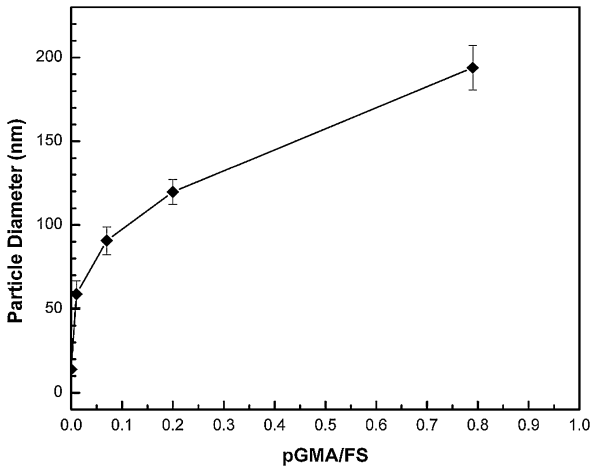

Fig. 4. Correlation between the particle diameters, determined by DLS, and the weight FS/pGMA ratio determined by TGA.

The average diameter and size-distribution of water suspension of the colloidal NPs were determined by DLS. The average diameters for the different preparation conditions changed from 195 nm to 60 nm with approximately 10% of standard error (Table 2). Fig. 1

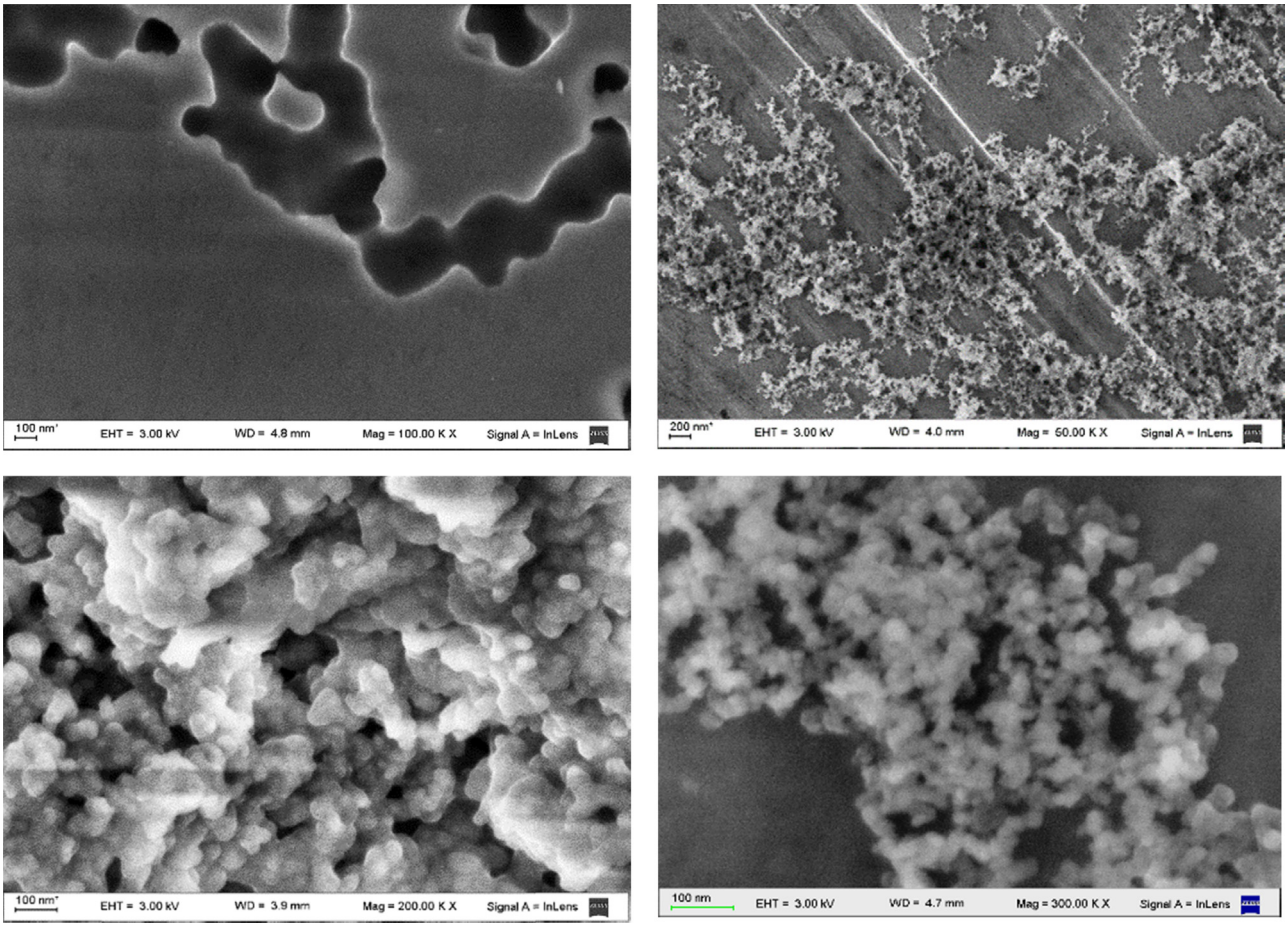

Fig. 5. FSEM microphotography of pGMA (up left; 100,000×); Bare fumed silica (up right; 60,000×); FS–pGMA composite (down left; 200,000×) and FS54/pGMA (down right; 300,000×).

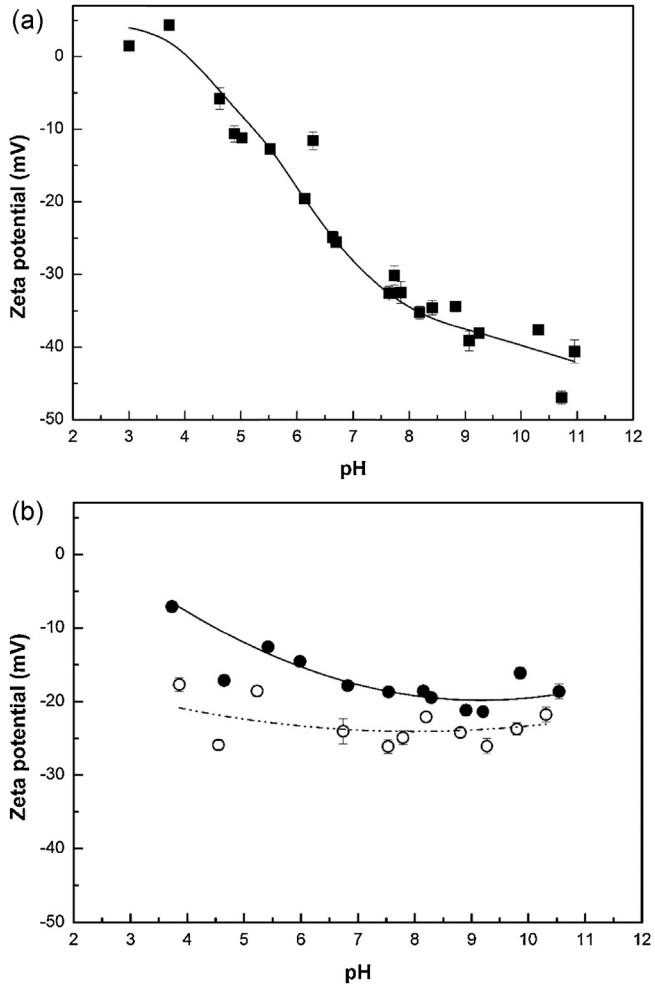

Fig. 6. Analysis of the *Z*-potential in the whole pH range for (a) FS and (b) S-FS9/pGMA.

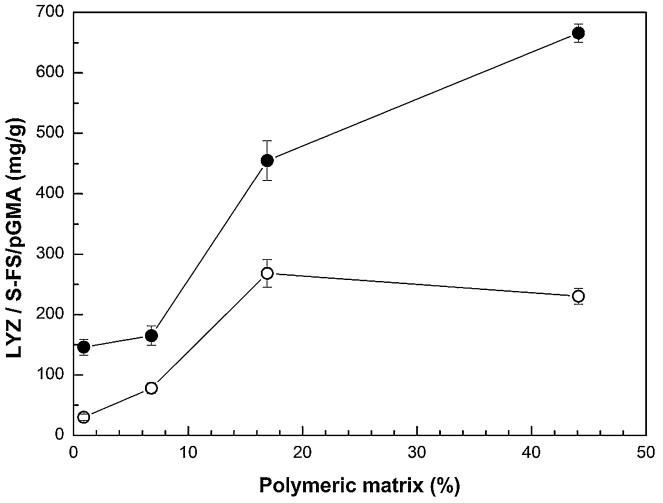

Fig. 7. Correlation between the protein adsorption capacity and the percentage of polymeric matrix in the colloidal composites. Maximum lysozyme adsorption (●) and maximum lysozyme capacity (○) as a function of amount of polymeric matrix percentage in NP composition.

shows the corresponding size-distribution histograms of the four samples prepared. According to the DLS data, the increase in the FS amount in the NP preparation yielded proportionally lower NP size, with a highly monodisperse size distribution.

Dry samples were characterized by FTIR spectroscopy using the ATR accessory. Fig. 2 shows the spectra corresponding to bare FS, the pGMA homopolymer and colloidal FS2/pGMA NP. The large peak at 1100–1000 cm^{-1} and the peak at 800 cm^{-1} in FS spectrum were assigned to the symmetric and asymmetric stretching vibrations of siloxane groups (Si—O—Si). Spectra corresponding to pGMA and FS/pGMA NPs show the characteristic stretching vibration of the carbonyl group at 1720 cm^{-1}, in addition to other small signals corresponding to the glycidylmethacrylate moieties such as CH, CH_3 and epoxy groups at 2950, 1445 and 900 cm^{-1} respectively [31].

The percentage of methacrylate polymer in the NPs was determined by TGA. Fig. 3 shows TGA plots of FS*x*/pGMA NPs after corrections of the water content. The region of weight loss (between 190 and 500 °C) shows two regions in most of the samples (see derivative plots in Fig. 3b), corresponding to the thermal oxidation and pyrolysis. Samples containing high FS/GMA ratios show progressive lower amounts of organic matter up to near 1% (w/w) content. In addition, the temperature required for the organic decomposition shows a shift to higher temperatures when the proportion of polymer in the sample decreases. The decomposition temperature corresponding to the FS2/pGMA sample begins at 230 °C. This transition range, about 100 °C lower than that of the other samples, has a profile similar to that of the free pGMA decomposition. In FS9/pGMA, FS27/pGMA and FS54/pGMA, the degradation process begins at 310–330 °C, indicating an increase in thermal stability, which is attributable mostly to an interaction with FS. This trend is also visible in the derivative plot of the degradation curves (Fig. 3b), which shows the corresponding degradation rates. In all cases, the decomposition process involves two well-defined stages: one (the more important) corresponding to the polymethacrylate depolymerization, and the other corresponding to the decomposition of the ester groups [32]. TGA also allowed estimating the composite composition, which varied from 44.1% to 0.9% of pGMA for FS2/pGMA to FS54/pGMA respectively.

Fig. 4 shows the NP data corresponding to DLS and TGA. The increase in the polymer ratio in the final NP composition yields a higher NP diameter. However, this correlation is not linear and approaches a plateau as the polymer mass increases.

Fig. 5 shows scanning electron microscopy micrographs of the pGMA homopolymer, bare FS NP and colloidal FS/pGMA NP corresponding to FS54/pGMA. Micrographs with different magnification are shown in order to visualize their characteristics and the uniformity over the whole field studied. However, no individual NPs were captured after the pre-drying process required to analyze the samples. FS/pGMA NP micrographs illustrate the homogeneity of the NP size, with an average NP diameter in the order of 30 nm, which is lower than the average particle size obtained by DLS (about 60 nm). This difference could be assigned to a swelling effect in the hydrated state.

Sulfonic groups were further introduced in the FS/pGMA NPs (S-FS/pGMA NPs) through a well-described reaction of sulfite onto the epoxy-pendant groups of pGMA. The negative surface change composition of the NPs was examined by zeta potential versus pH. Curves were recorded onto FS and FS9/pGMA and its sulfonate derivative (Fig. 6). Fig. 6a shows the FS curve decreasing with the pH with an isoelectric point at pH 3.5. The composite NP shows a flat curve between −5 mV and −20 mV in all the pH range. Its sulfonate derivative shows the same shape at more negative zeta potentials (between −20 mV and −30 mV), which can be assigned to the presence of sulfonic moieties in the polymeric matrix.

Based on the results achieved with the different techniques, we schematized a plausible sequence for the preparation of S-FS/pGMA NPs, considering the extreme conditions of FS/pGMA ratios, where

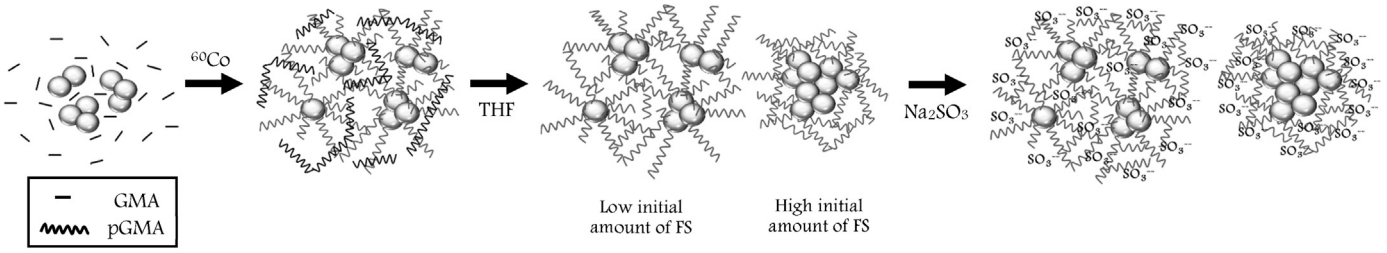

Fig. 8. Proposed scheme according to the experimental measurements determined onto the colloidal composites samples prepared from FS and GMA. From left to right: Bare FS dispersed in GMA solution; FS/pGMA composite after irradiation; FS/pGMA NP after extraction step (left: low initial amount of FS; right: high initial amount of FS and sulfonic FS/pGMA NP after chemical derivatization).

Table 3
Determination of protein adsorption properties of the sulfonic FS*x*/pGMA NPs. Maximum lysozyme adsorption (Ads_{max}) and maximum protein capacity (Q_{max}), determined as mg of lysozyme per gram of material.

Sample	Particle diameter (nm)	Ads_{max} (mg/g)	Q_{max} (mg/g)
S-FS2/pGMA	190	666 ± 15	230 ± 13
S-FS9/pGMA	120	455 ± 33	268 ± 23
S-FS27/pGMA	90	165 ± 16	78 ± 9
S-FS54/pGMA	60	146 ± 13	30 ± 5

lower relative amounts of FS allow reaching larger NP size dispersed in the hydrogel polymeric matrix (Fig. 7).

The anionic colloidal nanoparticles of different sizes, S-FS*x*/pGMA NPs, were used to capture a cationic protein, lysozyme, at neutral pH. It has been previously demonstrated that the interaction between negatively charged microgel particles and lysozyme occurs at low salt concentrations, in a fashion similar to that of micro-scale particles [33]. Here, we studied lysozyme adsorption to colloidal NPs using a protocol of four steps: equilibration, adsorption, washing and elution, where centrifugation is used for NP recovery. Table 3 shows the total adsorption (Ads_{max}) and maximum adsorption capacity (Q_{max}) of lysozyme from S-FS*x*/pGMA NPs. The adsorption capacity increased proportionally to the diameter of NPs. Therefore, a surface adsorption process was discarded and it can be assumed that S-FS/pGMA NPs have a hydrated gel structure with adsorption properties. This observation is also consistent with the variation in particle sizes obtained by DLS and FSEM. It has been reported that a sulfite add-on reaction onto surface-grafted pGMA materials leads to highly hydrated and hydrophilic matrixes [22]. Consequently, S-FS/pGMA NPs should have an adsorption behavior similar to that of polystyrene-polyacrylate core–shell microgels [34].

Fig. 8 shows the adsorption parameters (Ads_{max} and Q_{max}) versus the percentage of polymer in the NP composition. Up to around 20%, the adsorption capacity and the amount of polymer show a direct correlation. NPs with higher polymer proportions did not improve the maximum adsorption capacity, suggesting a different composite arrangement. A maximum of 270 mg/g of reversible adsorption of lysozyme per gram was achieved using NPs of 120 nm diameter and 44.1% of pGMA.

4. Conclusion

Preparation of novel colloidal FS/pGMA nanocomposite was achieved by a radiation-induced polymerization method. The gamma-ray irradiation of an aqueous solution of GMA, at low monomer concentration, with the presence of FS nanoparticles, allowed obtaining a monodisperse nanocomposite. These composite NPs, which ranged from 60 to 200 nm in diameter, contained approximately 55–99% of silica by mass. Particle size was inversely proportional to the initial FSi/GMA ratio, reaching a maximum of 44% pGMA in the colloidal composite.

Advantages of this preparation method include that it is a simple one-pot protocol based on readily available starting materials, that no addition of surfactant is necessary during the preparation, and that it is a non-stirring reaction. Also, no surface pretreatment of the FS is required, and the reactivity of GMA can be used for a wide-range of NP functionalization.

Sulfonic FS/pGMA NPs were able to absorb lysozyme reversibly up to 270 mg/g from an aqueous protein solution. This protein adsorption property, in addition to the simple recovery method of NPs, centrifugation, and non-toxic preparation materials, makes this colloidal nanocomposite an interesting adsorbent to be applied in the field of DSP of bioproducts.

Acknowledgments

MG and RC are members of the National Council of Scientific and Technical Research (CONICET), and LJM, MLS and PK would like to thank CONICET for their fellowships. The research leading to these results has received funding from the European Union Seventh Framework Programme (FP7/2007–2013) under grant agreement no. 312004 (INTENSO Project) and Argentinean grants from Ministry of Science, Technology and Productive Innovation (MINCYT) and Universidad Nacional de Quilmes (UNQ), Buenos Aires, Argentina.

References

[1] H. Zou, S.S. Wu, J. Shen, Polymer/silica nanocomposites: preparation, characterization, properties and applications, Chem. Rev. 108 (2008) 3893–3957.
[2] D.H. Yoona, J.W. Jangb, I.W. Cheonga, Synthesis of cationic polyacrylamide/silica nanocomposites from inverse emulsion polymerization and their flocculation property for papermaking, Colloids Surf. A: Physicochem. Eng. Aspects 411 (2012) 18–23.
[3] M. Demir, Y. Menceloglu, B. Erman, Effect of filler amount on thermoelastic properties of poly(dimethylsiloxane) networks, Polymer 46 (2005) 4127–4134.
[4] K. Zhang, L. Zheng, X. Zhang, X. Chen, B. Yang, Silica–PMMA core–shell and hollow nanospheres, Colloids Surf. A: Physicochem. Eng. Aspects 277 (2006) 145–150.
[5] M. Percy, J. Amalvy, C. Barthet, S. Armes, S. Greaves, J. Watts, H. Wiese, Surface characterization of vinyl polymer–silica colloidal nanocomposites using X-ray photoelectron spectroscopy, J. Mater. Chem. 12 (2002) 697–702.
[6] R. D'Souza, M. Azevedo, M. Aires-Barros, N. Lendero Krajnc, P. Kramberger, M.L. Carbajal, M. Grasselli, R. Meyer, M. Fernández-Lahore., Emerging technologies for the integration and intensification of downstream bioprocesses, Pharm. Bioprocess. 1 (2013) 423–440.
[7] F. Xu, J. Geiger, G. Baker, M. Bruening, Polymer brush-modified magnetic nanoparticles for his-tagged protein purification, Langmuir 27 (6) (2011) 3106–3112.
[8] X.Y. Liu, S.W. Zheng, R.Y. Hong, Y.Q. Wang, W.G. Feng, Preparation of magnetic poly(styrene-co-acrylic acid) microspheres with adsorption of protein, Colloids Surf. A: Physicochem. Eng. Aspects 443 (2014) 425–431.
[9] I. Fischer, C.C. Hsu, M. Gärtner, C. Müller, T.W. Overton, O.R. Thomas, M. Franzreb, Continuous protein purification using functionalized magnetic nanoparticles in aqueous micellar two-phase systems, J. Chromatogr. A 1305 (2013) 7–16.

[10] I. Safarik, M. Safarikova, Magnetic techniques for the isolation and purification of proteins and peptides, Biomagn. Res. Technol. 2 (7) (2004), http://dx.doi.org/10.1186/1477-044X-2-7.
[11] T. Brunner, P. Wick, P. Manser, P. Spohn, R. Grass, L. Limbach, A. Bruinink, W. Stark, In vitro cytotoxicity of oxide nanoparticles: comparison to asbestos, silica, and the effect of particle solubility, Environ. Sci. Technol. 40 (2006) 4374–4381.
[12] G. Liu, J. Gao, H. Ai, X. Chen, Applications and potential toxicity of magnetic iron oxide nanoparticles, Small 9 (2013) 1533–1545.
[13] Y. Park, H. Bae, Y. Jang, S. Jeong, H. Lee, W. Ryu, M. Yoo, Y. Kim, M. Kim, J. Lee, S. Wook Son, Effect of the size and surface charge of silica nanoparticles on cutaneous toxicity, Mol. Cell. Toxicol. 9 (2013) 67–74.
[14] S. Dekkers, H. Bouwmeester, P. Bos, R. Peters, A. Rietveld, A. Oomen, Knowledge gaps in risk assessment of nanosilica in food: evaluation of the dissolution and toxicity of different forms of silica, Nanotoxicology 7 (4) (2013) 367–377, http://dx.doi.org/10.3109/17435390.2012.662250.
[15] A. Nieto, S. Areva, T. Wilson, R. Viitala, M. Vallet-Regi, Cell viability in a wet silica gel, Acta Biomater. 5 (2009) 3478–3487.
[16] H. Sugimoto, K. Daimatsu, E. Nakanishi, Y. Ogasawara, T. Yasumura, K. Inomata, Preparation and properties of poly(methylmethacrylate)–silica hybrid materials incorporating reactive silica nanoparticles, Polymer 47 (2006) 3754–3759.
[17] K. Naitoh, K. Koseki, T. Yamaoka, An aqueous-base developable photoresist based on light-induced cationic polymerization – resist performance of poly(glycidyl methacrylate-comethacrylic acid), J. Appl. Polym. Sci. 50 (1993) 243–250.
[18] A. Hayek, Y.G. Xu, T. Okada, S. Barlow, X.L. Zhu, J.H. Moon, S.R. Marder, S. Yang, Poly(glycidyl methacrylate)s with controlled molecular weights as low-shrinkage resins for 3D multibeam interference lithography, J. Mater. Chem. 18 (2008) 3316–3318.
[19] M. Demir, G. Ugur, M. Gulgun, Y. Menceloglu, Glycidyl-methacrylate-based electrospun mats and catalytic silver nanoparticles, Macromol. Chem. Phys. 209 (2008) 508–515.
[20] T. Kawaia, K. Saitoa, W. Leeb, Protein binding to polymer brush, based on ion-exchange, hydrophobic, and affinity interactions, J. Chromatogr. B 790 (2003) 131–142.
[21] X.J. Song, J. Hu, C.C. Wang, Synthesis of highly surface functionalized monodispersed poly(St/DVB/GMA) nanospheres with soap-free emulsion polymerization followed by facile click chemistry with functionalized alkylthiols, Colloids Surf. A: Physicochem. Eng. Aspects 380 (2011) 250–256.
[22] M. Ventura, M. Fernandez Lahore, E.E. Smolko, M. Grasselli, High-speed protein purification by adsorptive cation-exchange hollow-fiber cartridges, J. Membr. Sci. 321 (2008) 350–355.
[23] B. Radhakrishnan, R. Ranjana, W. Brittain, Surface initiated polymerizations from silica nanoparticles, Soft Matter 2 (2006) 386–396, S.
[24] E. Bourgeat-Lami, in: H.S. Nalwa (Ed.), Encyclopedia of Nanoscience and Nanotechnology, vol. 8, American Scientific Publishers, Stevenson Ranch, CA, 2004, pp. 305–332.
[25] J. Amalvy, M. Percy, S. Armes, H. Wiese Synthesis, Characterization of novel film-forming vinyl polymer/silica colloidal nanocomposites, Langmuir 17 (2001) 4770–4778.
[26] A. Henglein, D. Meisel, Radiolytic, Control of the size of colloidal gold nanoparticles, Langmuir 14 (1998) 7392–7396.
[27] M. Grasselli, A. Navarro del Cañizo, S. Camperi, F. Wolman, E. Smolko, O. Cascone, Immobilized metal ion affinity hollow-fibre membranes obtained by the direct grafting technique, Radiat. Phys. Chem. 55 (1999) 203–208.
[28] E. Gachard, H. Remita, J. Khatouri, B. Keita, L. Nadjo, J. Belloni, Radiation-induced and chemical formation of gold clusters, N. J. Chem. 22 (1998) 1257–1265.
[29] D. Meisel, Basics of Radiation Chemistry in the Real World: Nanoparticles in Aqueous Suspensions. Advances in Radiation Chemistry of Polymers, 2004.
[30] M. Grasselli, N. Hargittai, A. Safrany, E. Smolko, From microspheres to monoliths: synthesis of porous supports with tailored properties by radiation polymerization, Nucl. Instrum. Methods Phys. Res. B 185 (2001) 254–261.
[31] D. Lin-Vien, N. Colthup, W. Fateley, J. Grasselli, The Handbook of Infrared and Raman Characteristics Frequencies of Organic Molecules. London, 1991.
[32] S. Zulfiqar, M. Zulfiqar, I. Nawaz, I. McNeill, J. Gorman, Thermal-degradation of poly(glycidyl methacrylate), Polym. Degrad. Stabil. 30 (1990) 195–203.
[33] C. Johansson, P. Hansson, M. Malmsten, Interaction between lysozyme and poly(acrylic acid) microgels, J. Colloid Interface Sci. 316 (2007) 350–359.
[34] N. Welsch, A.L. Becker, J. Dzubiella, M. Ballauff, Core–shell microgels as smart carriers for enzymes, Soft Matter 8 (2012) 1428–1436.